

# Analysis of the Low Frequency Shielding Behavior of High Voltage Cables in Electric Vehicles

Katharina Feldhues, Maja Diebig, Stephan Frei

TU Dortmund University

Dortmund, Germany

katharina.feldhues@tu-dortmund.de

**Abstract—** In this paper the low frequency shielding behavior of shielded high voltage cables for electric vehicles is analyzed using analytical methods. First the basic theory on the operational modes and modeling of cables is presented. Measurements and numerical simulations are done to verify the models. The powertrain of an electric vehicle is investigated using the simulation models. A parametrical study determines the influence of parameters such as height and distance of the cables and gives information for an EMC compliant layout. The magnetic fields for different cable setups are calculated and compared with values from health protection standards.

**Index Terms—**Shielded Cables, Electric Vehicle, Low Frequency Magnetic Field, ICNIRP

## I. INTRODUCTION

To reduce the magnetic field from cable systems different methods can be used, e.g. changing the order of the cables or using shielded cables. Especially for the drive chain in electric vehicles shielded cables are utilized. While communication coaxial cables use the shield as the return path, for shielded power cables the shield is not intended as the current return path. Hence the shield cannot compensate the resulting magnetic field to zero. All the mentioned effects have to be considered. In this paper a low frequency model for shielded cables is presented. With this model the current distribution and the shielding efficiency can be calculated with a circuit solve. Assuming a homogeneous cable configuration and the validity of the superposition theorem the magnetic flux density can be computed with analytical approaches.

The paper is structured as follows. In chapter II the calculation of per-unit-length (p.u.l.) parameters for low frequency analyses of shielded cables is discussed. With these p.u.l. parameters a low frequency model is generated. For validation, measurements are done and the results are compared with the simulation (chapter II.B). In chapter IV the developed model is used for determining the shield currents in a propulsion system. Geometry parameters are varied to identify critical configurations. The magnetic flux density is calculated for different setups. With these investigations recommendations for the layout of shielded cables were derived.

## II. SHIELDED CABLES AT LOW FREQUENCIES

In this section a circuit model for a set of shielded cables is presented. The model is explained exemplarily for a system with two shielded cables above ground plane. A typical automotive

HV cable shield can be treated as solid shield up to approximately 1 MHz. As seen in [1] up to this frequency range the dc resistance is the dominant parameter. Shown results are considered to be valid up to 1 MHz.

### A. Derivation of the Cable Model

Figure 1 shows a two cable system above a ground plane which is used for the return path. Therefore the system can be divided into five conductors, the two inner cables, the two shields, and the ground plane. Hence, the system can be regarded as a multi conductor transmission line.

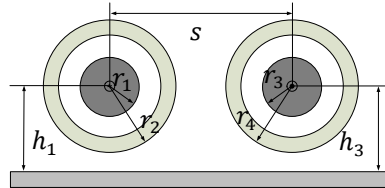


Figure 1. System with two shielded cables above a ground plane

### 1) Calculating the Inductances

For a multi conductor system the p.u.l. self-inductance  $L_{ii}$  of each cable can be calculated according to [2]:

$$L_{ii} = \frac{\mu_r \cdot \mu_0}{2\pi} \cdot \operatorname{arccosh}\left(\frac{h_i}{r_i}\right) \quad (1)$$

The p.u.l. self-inductance of the shield  $L_{ii}$  is calculated here as the self-inductance of a solid wire, see equation (1), with the outer radius of the shield for the radius  $r_i$ . This approach can be used because the magnetic flux density, needed for calculating the self-inductance of a hollow cylinder, is the same as for a solid cylinder. For the calculation of the mutual p.u.l. inductivity  $L_{ij}$  the coupling path has to be regarded. This is the same coupling path as for the shield. Therefore the mutual inductance is the same as the self-inductance of the shield [3].

$$L_{ij} = L_{jj} = \frac{\mu_r \cdot \mu_0}{2\pi} \cdot \operatorname{arccosh}\left(\frac{h_j}{r_j}\right) \quad (2)$$

Considering a coaxial layout the mutual inductances between the inner conductors  $L_{ij}$  are the same for each wire. They only depend on the location of the center and the distance between the inner conductors  $s_{ij}$  [3].

$$L_{ij} = \frac{\mu_r \cdot \mu_0}{4\pi} \cdot \ln\left(1 + 4 \frac{h_i h_j}{s_{ij}^2}\right) \quad (3)$$

## 2) Calculating the Capacities

For lower frequencies the shield can be regarded as perfect, therefore some capacities can be set to zero. No direct capacitive coupling is possible from the inner conductor to other cables or to the ground plane. The capacity between the inner wire and the shield can be calculated using [3]:

$$C_{ij} = \frac{2\pi \cdot \epsilon_r \cdot \epsilon_0}{\ln(r_j/r_i)} \quad (4)$$

With the assumption that the surrounding medium is homogeneous the following relation can be used [2]:

$$[C] = \mu_0 \mu_r \epsilon_r \epsilon_0 [L]^{-1}. \quad (5)$$

## 3) Calculating the Resistance

The per-unit-length resistance can be calculated with equation (6) depending on the conductivity  $\sigma_i$  and the cross section  $A$  of the cable. The skin effect and the proximity effect are neglected due to the considered low frequency range [4].

$$R_{DC\_i} = \frac{1}{\sigma_i \cdot A}. \quad (6)$$

With these parameters a low frequency simulation model can be generated. The resulting equivalent circuit is shown in Fig. 2.

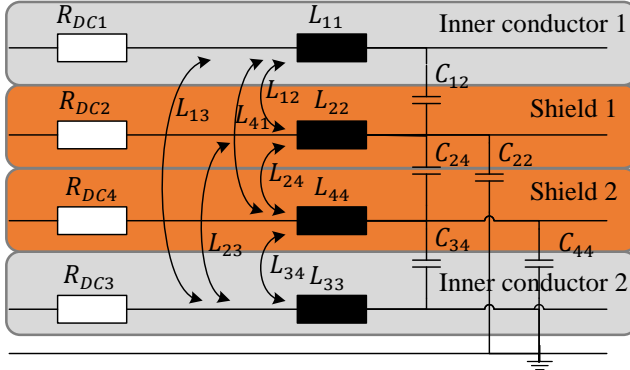


Figure 2. Circuit model of two shielded cables above ground

## B. Calculation of the Magnetic Flux Density

In this paper the magnetic flux density is calculated with an analytical approach to reduce the calculation time and simplify parameter variations. For this approach it is assumed that the current distribution is homogeneous. The magnetic flux density is calculated with the common formula:

$$B = \mu \cdot \frac{I}{2 \cdot \pi \cdot r}. \quad (7)$$

In order to analyze a cable system above the metallic car body the image theory was investigated with numerical calculations using FEM [5]. For comparisons a single wire above ground was considered. The configuration is shown in Fig. 3.

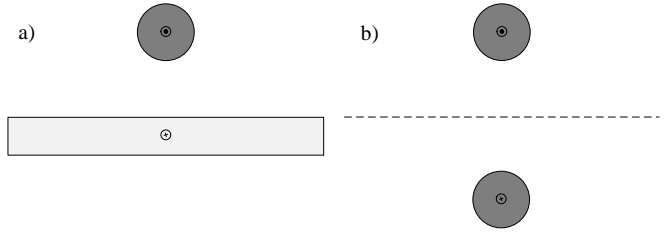


Figure 3. Schematic layout for numerical calculation  
a) single wire above ground b) image theory

Several points around the cables were analyzed. In Fig. 4 the deviation of the results for different frequencies for the magnetic flux density for both setups is shown.

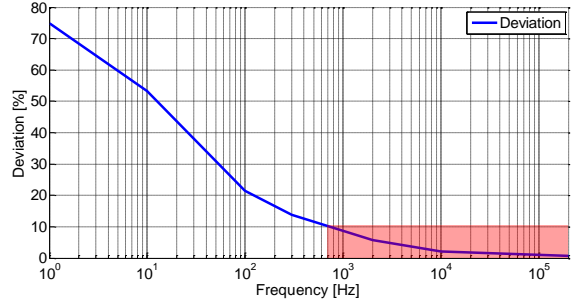


Figure 4. Deviation “single wire above solid copper ground” - “image theory”

For low frequencies the deviation is higher due to the current density of an infinite long solid ground plane which is almost zero. As shown in Fig. 4 for frequencies above 700 Hz the deviation is smaller than 10 %. At several tenth Hz the deviation is less than 3 dB so the image theory can be used for a wide frequency range.

## III. VERIFICATION OF CABLE MODEL

In this chapter the results of the simulation are compared to measurements. Two application cases are analyzed.

### A. Measurement Setup

A vector network analyzer (VNA) is used to measure the scattering parameters. The measurement is realized with the setup shown in Fig. 5. The measurement setup is located on a copper plane. The VNA is isolated from the ground plane.

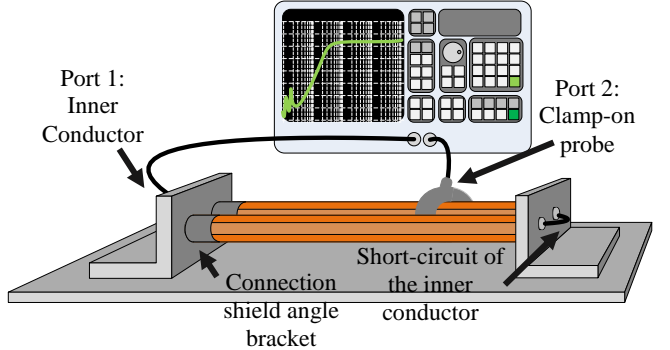


Figure 5. Measurement setup

For the measurement the shield is connected to two metallic brackets. To separate both circuits the brackets are directly connected to the ground plane. Therefore the shields have the ground plane as the return path. The inner conductors are short-circuited. One port of the VNA is connected to the first port and impresses a current. The inner wire is used as the return path. The current probe is connected to the second port of the VNA. All presented results are based on an excitation current of 1 A.

### B. System of Two Shielded Cables

In this test case the setup described in part II (Fig. 5) is analyzed. The comparison between the simulation and measurement is shown in Fig. 6.

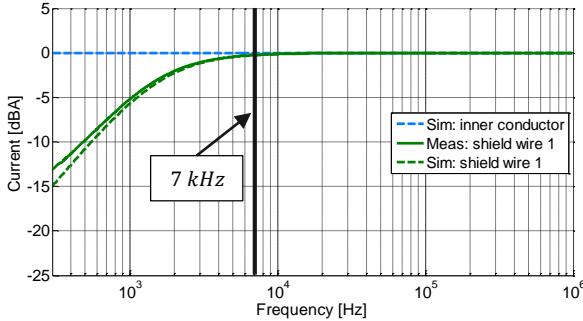


Figure 6. Simulation vs. measurement – two shielded cables

The ratio between the inner conductor current  $I_i$  and the shield current  $I_s$  can be calculated with the shield inductance  $L_S$  and the DC resistance  $R_{DCS}$  of the shield.

$$\frac{I_s}{I_i} = \frac{j\omega L_S}{(j\omega L_S + R_{DCS})} \quad (8)$$

For lower frequencies the dominant parameter is the DC resistance as seen in (8). With increasing frequency the influence of the inductance grows. The shield current and the inner conductor current are the same when the impedance of the inductance is greater than the ohmic resistance ( $j\omega L_S \gg R_{DCS}$ ). For the analyzed setup this frequency is  $f \gg 1 \text{ kHz}$ . As shown in Fig. 6 for frequencies above 7 kHz the current on the inner wire is nearly the same as on the shield. Hence the field is well compensated.

### C. Three Shielded Cables

For the connection between the motor and the power electronics three shielded cables are necessary. A setup with three wires in a flat (Fig. 7 a)) or a triangular layout (Fig. 7 b)) can be used. The simulation models can be generated in the same way as described in chapter II.

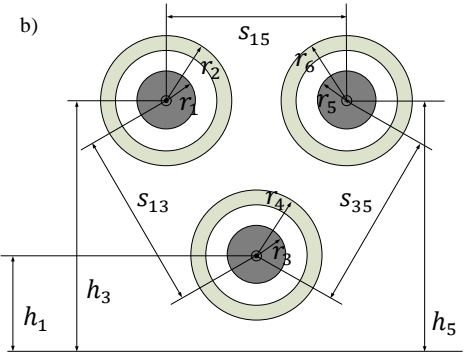
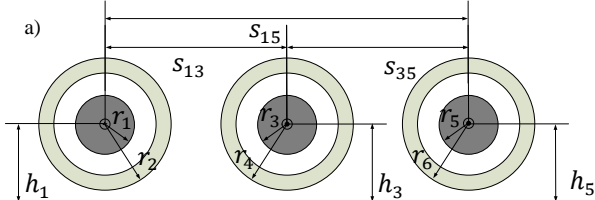


Figure 7. System with three shielded cables in a)flat and b)triangular setup

To validate the simulation model with measurements a current is impressed in one cable and the other two cables are used for the return current. In the first case only the center cable is excited. Therefore the system can be described as symmetric and the currents on the other wires are the same. For the second case one of the outer cables is connected to a current source defining an unsymmetrical case.

#### 1) Three Shielded Cables – Flat Layout

The first investigations are made with the symmetrical setup as shown in the upper part of Fig. 7. The return current is carried on two wires therefore the current on both wires is the same. Fig. 8 shows the results of measurement and the simulation. Due to the split of the return path the cables carry only half of the current (-6dB).

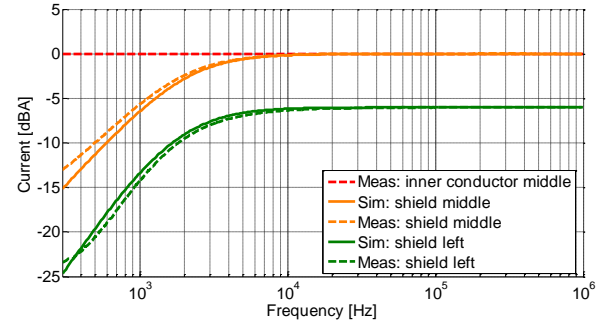


Figure 8. Simulation vs. measurement – excitation of middle wire

Due to the same geometrical structure the frequency is the same as for the two cables. The difference between the measurement and the simulation is small.

#### 2) Three Shielded Wires – Triangular Layout

For the triangular layout (see Fig. 7)) an unsymmetrical case is analyzed. One of the upper shielded cables is excited. The currents in both return paths are different for lower frequencies. Fig. 9 shows almost no deviation between the simulation and measurement results.

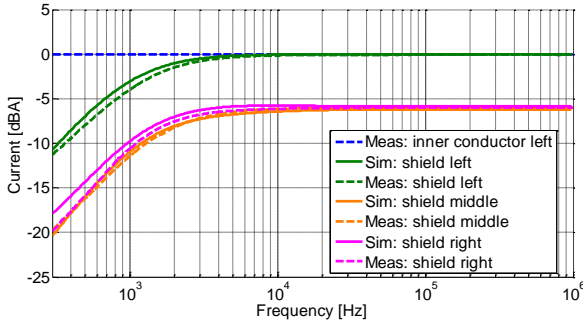


Figure 9. Simulation vs. measurement – excitation of left wire

#### IV. APPLICATION

##### A. Supply Line – Influence Of The Position

For the first application case a two cable configuration above ground (Fig. 10) is considered as it can be found between the battery and the power electronics.

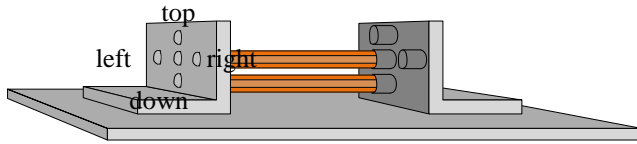


Figure 10. Application Case I – schematic

The influence of the arrangement of the wires is investigated by analyzing a parallel to ground (left and right) and orthogonal to ground (down and top) cable arrangements. The distance between the two cables is 5 cm. The excited cable is 5 cm above ground and the position of the return path is varied.

For the two positions parallel to round plane (left and right) the results are equal because the height above ground and distance between the cables are the same. Switching the excitation and return path of the cable does not influence the inductive coupling to the shield.

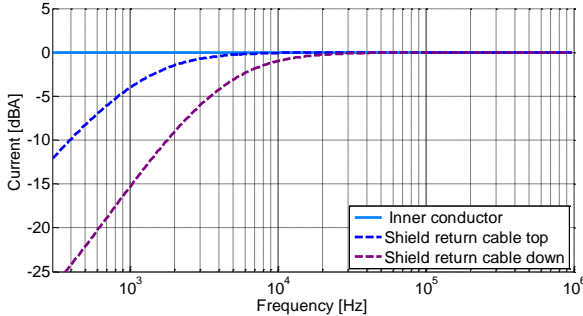


Figure 11. Simulation of DC cables vertical position

For the vertical case (see Fig. 11) differences occur due to the changing of the height. Is the return path located under the cable the difference between both shield currents is the maximum.

##### B. Powertrain

In the next application case a simple powertrain in electrical vehicles, as shown in Fig. 12, is assumed. The cables between the power electronics and the electric machine are investigated.

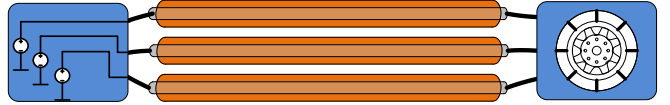


Figure 12. Application case II–schematic

The output of the inverter is simulated with three current sources with an amplitude of 200 A. The phases are shifted with 0° for the cable in the middle and 120° and 240° for the cables on the left and right side.

##### 1) Parametrical Studies

For the parametrical studies the two layouts (flat and triangular) from section III.C are analyzed. The shield current is normalized to the inner conductor current. For each setup, cross section, height, or distances of the wires are varied. In the triangular order an isosceles triangle is generated. The height of the wire in the middle is varied. Hence the height of the other two cables is calculated depending on the height of the middle cable. When varying the cross section the cables are located 5 cm above ground and the distance between the cables is 5 cm. The simulation is done with four standardized cross sections (16, 25, 35, 50 mm²). Varying the cross section leads to a maximal difference of 5 dB. Hence it can be said that the influence of the cross section is small.

The influence of the distance and height is investigated for a 35 mm² cable. To compare the results the cut-off frequency (3 dB) is determined. The cut-off frequency is defined at the point where the deviation of the inner wire and the shield current is 3 dB. For both layouts the results (flat and triangular) are similar. Hence only the simulation results for the flat order are shown in Figure 13.

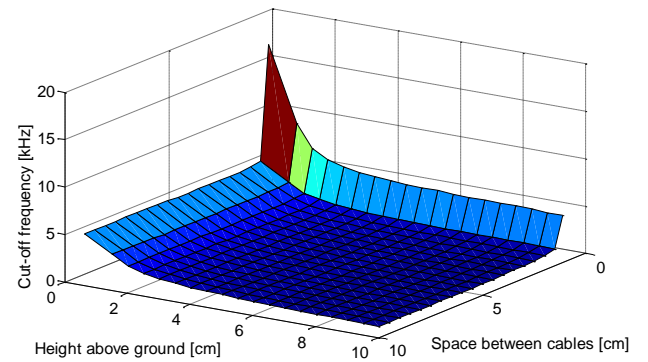


Figure 13. Cut-off frequency depending on distance and height

A greater distance between the wires generates a lower cut-off frequency. When only the inner conductor and shield current is considered the conclusion is, that minimum cut-off frequency requires a great distance between and a great height above ground.

## 2) Magnetic Flux Density and Health Protection Thresholds

For comparing to health protection thresholds the magnetic flux density must be known. Different investigations on the magnetic fields for low frequency systems were published, e.g. [6–9]. In most publications the ground plane is not considered [7]. In [8] it was stated that the magnetic field generated from a flat cable configuration is higher than of a triangular configuration. For an electric vehicle a flat configuration may be most likely because of the limited installation space in the vehicle.

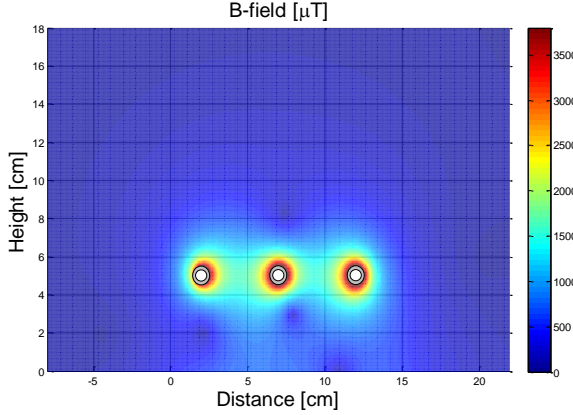


Figure 14. Magnetic flux density

For calculating the magnetic flux density with the analytical approach the conductor and shield current sum up to the common mode current. This current is a line source current for the magnetic field. In Fig. 14 the magnetic flux density for three cables above ground is shown. The simulation is done with a  $35 \text{ mm}^2$  cable with  $200 \text{ A}$  at a frequency of  $2 \text{ kHz}$ . Analytical field computation was compared to a finite element numerical computation [5]. The deviation is less than  $3 \text{ dB}$ .

The field in a distance of  $50 \text{ cm}$  is calculated and shown in Fig. 15.

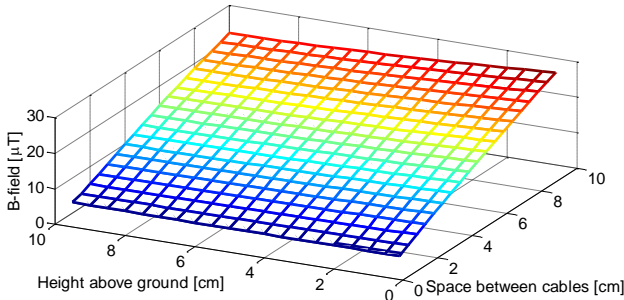


Figure 15. Influence on magnetic field flat order

As shown in Fig. 15 a) for the flat cable configuration the influence of the distance between the cables is higher than the influence of the height. To minimize the magnetic flux density around the cables the distance between the cables and the height above ground has to be minimal. For the triangular structure both parameters influence the resulting field in the same way.

Here it can be noted that the shield does not have to carry the whole return current to minimize the electromagnetic emission. The order of the cables also influences the resulting field. As shown in Fig. 15 for the horizontal order with decreasing the height and distance between the cable the resulting magnetic flux density is also decreasing. This leads to the known conclusion that the optimal layout requires small distances and heights.

Thresholds for health protection could be found in several standard, e.g. [10–13]. The operating frequency of a powertrain system in an electrical vehicle is in the frequency range of  $0 \text{ Hz}$  up to  $2 \text{ kHz}$ . The maximum threshold values are between  $160 \mu\text{T}$  for  $500 \text{ Hz}$  and  $41 \mu\text{T}$  for  $2 \text{ kHz}$ . The minimal emission for the flat layout is generated when all wires are directly positioned on the ground plane and directly next to each other. The simulation is done with a  $35 \text{ mm}^2$  cross section cable and  $200 \text{ A}$  current in a distance of  $50 \text{ cm}$  from the ground plane. The thresholds from [11] are the lowest limits so the simulation results are compared with these values.

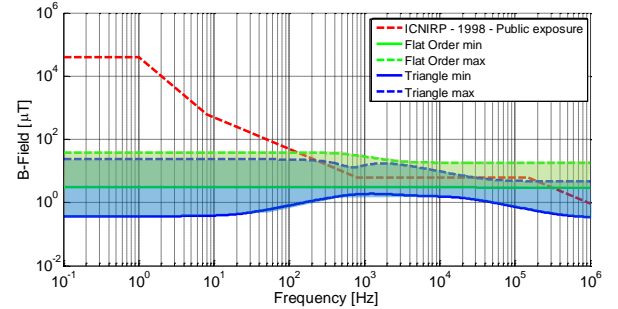


Figure 16. Comparision of thresholds and simulated field at  $50 \text{ cm}$  distance

In Fig. 16 the comparison of the calculated magnetic flux densities are shown. The thresholds from [11] are not reached for both setups with minimal height and distance between cables. Using assumed maximal values for height and space between cables the thresholds are violated. With the focus on the whole frequency range, for the minimal flat order are not reached up to  $300 \text{ kHz}$ . When using the maximal values the limits are already reached at  $200 \text{ Hz}$ .

For lower frequencies the curve is constant for the flat cable arrangement because the induced shield currents are low and only the inner conductor currents are visible. With increasing frequencies the shield current rises which leads to a decreasing B-field up to the point when the shield current is nearly equal to the inner conductor current. For higher frequencies only the return current influences the magnetic flux density. Therefore the field is lower.

In the triangle order the interpretation is more complex. Due to the fact of different heights the system consists out of different inductivities. This leads to a compensation between the shield and inner conductor currents at different frequency points. Hence the resulting magnetic field is a superposition of these effects.

## V. SUMMARY AND OUTLOOK

In this paper the theory of shielded cables for lower frequencies is analyzed. Analytical simulation models for currents and magnetic fields were created and verified with measurements and numerical simulations.

In the simulation the shield currents and the return paths for the shield currents were considered. Due to the special electric vehicles operation mode, the shielded cables cannot ensure significant magnetic field strength reduction in the cable environment.

The analytical magnetic flux density calculation is based on mirror theory. To validate this approach it was compared to a numerical calculation. This comparison shows that for frequencies above 700 Hz the analytical approach is sufficiently accurate. For three shielded cables above ground as used for a powertrain the best layout for the cables is directly on the ground plane with minimum distance to each other.

The analytical approach allows to calculate the magnetic flux density in a faster way than the numerical calculation. Hence parameter variation can be done in shorter time.

In future work a not ideal ground plane should be analyzed further. Moreover more parameter studies will be done. With the result additional rules for routing of the shielded cables in electric vehicles can be found.

## ACKNOWLEDGEMENT

The work in this paper was partly funded by the European Union (EFRE), the North Rhine-Westphalian Ministry for Economic Affairs, Energy, Building, Housing and Transport and the North Rhine-Westphalian Ministry for Climate Protection, Environment, Agriculture, Conservation and Consumer Affairs as part of the TIE-IN project.

## REFERENCES

- [1] A. Mushtaq, S. Frei, K. Siebert, and J. Bärenfänger, “Analysis of shielding effectiveness of HV cable and connector systems used for electric vehicles,” in *Electromagnetic Compatibility (EMC EUROPE), 2013 International Symposium on*, 2013, pp. 241–246.
- [2] C. R. Paul, *Analysis of multiconductor transmission lines*. New York, NY [u.a.]: Wiley, 1994.
- [3] C. R. Paul, *Introduction to electromagnetic compatibility*, 2nd ed. Hoboken, NJ: Wiley, 2006.
- [4] F. M. Tesche, M. Ianoz, and T. Karlsson, *EMC analysis methods and computational models*. New York: John Wiley & Sons, 1997.
- [5] *QuickField: Finite Element Analysis System*: Tera Analysis Ltd.
- [6] R. G. Olsen, D. Deno, R. S. Baishiki, and J. R. Abbot, et al, “Magnetic fields from electric power lines: theory and comparison to measurements,” *Power Delivery, IEEE Transactions on*, vol. 3, no. 4, pp. 2127–2136, <http://ieeexplore.ieee.org/stamp/stamp.jsp?arnumber=194025>, 1988.
- [7] M. D’Amore, E. Menghi, and M. S. Sarto, “Shielding techniques of the low-frequency magnetic field from cable power lines,” in *Electromagnetic Compatibility, 2003 IEEE International Symposium on*, 2003, pp. 203–208.
- [8] M. D’Amore, D. Paladino, and M. S. Sarto, “New double-shielded power cables generating low magnetic field levels,” in *Electromagnetic Compatibility, 2005. EMC 2005. 2005 International Symposium on*, 2005, pp. 179–184.
- [9] M. A. Prsa, N. D. Micalica, and K. K. Kasas Lazetic, “Determination of electromagnetic field in a three-phase system with three single-core power electric cables 110 KV,” in *EUROCON 2009, EUROCON ’09*. IEEE, 2009, pp. 2040–2045.
- [10] “IEEE Standard for Safety Levels With Respect to Human Exposure to Electromagnetic Fields, 0-3 kHz,” *IEEE Std C95.6 2002*, pp. 0\_1, <http://ieeexplore.ieee.org/stamp/stamp.jsp?arnumber=1046043>, 2002.
- [11] International commission on non-ionizing radiation protection, *ICNIRP GUIDELINES 1998: For limiting exposure to time-varying electric, magnetic and electromagnetic fields (up to 300 GHz)*.
- [12] International commission on non-ionizing radiation protection, *ICNIRP GUIDELINES 2010: For limiting exposure to time-varying electrical and magnetic fields (1 Hz-100kHz)*.
- [13] *BGV B11 Elektromagnetische Felder*.